Quaternary Science Reviews 210 (2019) 164–174

Contents lists available at ScienceDirect

Quaternary Science Reviews

journal homepage: www.elsevier.com/locate/quascirev

Multiple sources for tephra from AD 1259 volcanic signal in Antarctic ice cores

Biancamaria Narcisi [a, *], Jean Robert Petit [b], Barbara Delmonte [c], Valentina Batanova [d], Joël Savarino [b]

[a] ENEA, C.R., Casaccia, 00123, Roma, Italy
[b] Univ. Grenoble Alpes, CNRS, IRD, Grenoble INP, IGE, 38000, Grenoble, France
[c] Department of Earth and Environmental Sciences (DISAT), Univ. Milano-Bicocca, Piazza della Scienza, 20126, Milano, Italy
[d] Univ. Grenoble Alpes, Univ. Savoie Mont Blanc, CNRS, IRD, IFSTTAR, ISTerre, 38000, Grenoble, France

ARTICLE INFO

Article history:
Received 10 January 2019
Received in revised form
22 February 2019
Accepted 4 March 2019

Keywords:
Cryptotephra
Antarctica
Ice cores
Volcanic isochron
Glass shard microanalysis
Antarctic rifting volcanism
Samalas AD 1257 eruption

ABSTRACT

Strong volcanic signals simultaneously recorded in polar ice sheets are commonly assigned to major low-latitude eruptions that dispersed large quantities of aerosols in the global atmosphere with the potential of inducing climate perturbations. Parent eruptions responsible for specific events are typically deduced from matching to a known volcanic eruption having coincidental date. However, more robust source linkage can be achieved only through geochemical characterisation of the airborne volcanic glass products (tephra) sometimes preserved in the polar strata. We analysed fine-grained tephra particles extracted from layers of the AD 1259 major bipolar volcanic signal in four East Antarctic ice cores drilled in different widely-spaced locations on the Antarctic Plateau. The very large database of glass-shard geochemistry combined with grain size analyses consistently indicate that the material was sourced from multiple distinct eruptions. These are the AD 1257 mega-eruption of Samalas volcano in Indonesia, recently proposed to be the single event responsible for the polar signal, as well as a newly-identified Antarctic eruption, which occurred in northern Victoria Land in AD 1259. Finally, a further eruption that took place somewhere outside of Antarctica has also contributed to tephra deposition. Our high-resolution, multiple-site approach was critical for revealing spatial heterogeneity of tephra at the continental scale. Evidence from ice-core tephra indicates recurrent explosive activity at the Antarctic volcanoes and could have implications for improved reconstruction of post-volcanic effects on climate from proxy polar records.

1. Introduction

Continuous volcanic profiles from polar ice sheets reconstructed by electric conductivity (ECM) and sulphate measurements are punctuated by prominent spikes recording explosive eruptions of the past (e.g., Hammer, 1980; Delmas et al., 1992; Langway et al., 1995; Severi et al., 2012; Sigl et al., 2014, 2015). These signals can be used both as reference horizons to provide independent age constraints for the ice core series, and to reconstruct the history of explosive volcanism and its relationship with climate. Volcanic events with bipolar occurrence are particularly interesting in this respect. These are typically interpreted as related to massive low-latitude events capable of producing sulphuric acidic deposition all over the world with the potential of forcing global climate (e.g., Langway et al., 1995; Sigl et al., 2015). Their record in both polar regions also enables direct north-south synchronisation of ice stratigraphies, which is of crucial importance to reconstruct the phasing of climatic events and understanding underlying mechanisms (Svensson et al., 2013).

Among the most outstanding volcanic deposition events of the last 2 millennia (Sigl et al., 2014), peak fallout of volcanic aerosols over the poles dated as AD 1259 represents a fundamental age marker for ice chronologies. Its signal is recorded in several Greenland and Antarctic ice cores, and was initially identified by Langway et al. (1988), who suggested that the parent volcano could be probably located in the Northern Hemisphere close to Equator. Since then, numerous papers have considered various aspects of this event (e.g. Delmas et al., 1992; Zielinski, 1995; Stothers, 2000).

* Corresponding author.
E-mail address: biancamaria.narcisi@enea.it (B. Narcisi).

https://doi.org/10.1016/j.quascirev.2019.03.005
0277-3791/

Particularly, its source has been a matter of debate as until recently no record of large volcanic eruption around that date was known. On the basis of analysis of tiny glass shards, Palais et al. (1992) suggested that the material from Greenland and South Pole (SP) ice core samples is indeed from the same volcano, and identified El Chichón, Mexico, as the probable source, despite the chemical match was not perfect in detail. Oppenheimer (2003) presented the hypothesis of a super-eruption of global significance or a smaller eruption enriched in sulphur. Baroni et al. (2008) used sulphur isotope analysis to indicate a stratospheric nature for the volcanic signals at the Antarctic Dome C and SP sites. More recently, a major caldera explosive event was identified at Samalas volcano, on Lombok Island, Indonesia (Lavigne et al., 2013; Vidal et al., 2015, 2016; Alloway et al., 2017). Based upon chronostratigraphic and geochemical studies nearby the source, and the analysis of historical texts, this eruption of exceptional size was dated at AD 1257, placed at the end of the Medieval Warm Period (ca. 900–1250 A.D., Mann et al., 2009). It has been inferred to be the single counterpart of the AD 1259 bipolar spike. In particular, according to a recent reconstruction of Antarctic continental-scale volcanic aerosol deposition, the sulphate injection greatly exceeded that of the AD 1815 cataclysmic Tambora eruption (Sigl et al., 2014).

When strong explosive volcanic eruptions occur, large quantities of solid particles (tephra) and gases penetrate the tropopause and rise to altitudes well within the stratosphere, where they can be distributed all around the globe. Tephra fallout can affect vast regions, and small particles can be deposited thousands of kilometres from active sources forming invisible horizons (e.g., Lowe, 2011; Ponomareva et al., 2015, and references therein). The fingerprint of volcanic material preserved in distant sites can univocally identify source areas and could be employed to disentangle the origin of volcanic glacio-chemical signals in polar ice cores (e.g., Yalcin et al., 2006; Dunbar et al., 2017), that otherwise is conjectured from the record of documented eruptions. However, especially for tropical-equatorial eruptions the amount of tephra that could be dispersed towards the poles is typically very small and the material very fine-grained, making such tephra study very challenging.

A preliminary exploratory investigation of a shallow Antarctic ice core from the Concordia-Dome C site revealed evidence of an appreciable concentration of cryptotephra in connection with the AD 1259 sulphate peak (Petit et al., 2016). This intriguing observation prompted us to carry out a detailed tephra study in order to make inferences about source(s) that produced the tephra and to discuss the related atmospheric implications. In this work we describe the characteristics of the glassy volcanic material associated with the AD 1259 signal in different sectors of the East Antarctic Plateau (EAP). We took advantage of having access to various good-quality ice cores covering the last millennium to apply a multiple core approach that allows highlighting the spatial distribution of volcanic products. Note that while attempts to identify the parent eruption of major polar signals through a tephra study often rely on few shards (e.g., Zielinski et al., 1997; Barbante et al., 2013), here we obtained a large dataset based on a considerable amount of electron probe microanalyses that allows recognizing compositional heterogeneities within tephra, in association with ash grain size measurements. We also considered an inventory of candidate source volcanoes more extended than that employed in previous studies.

2. Materials and methods

In this study we used 4 EAP ice cores located at elevations between 1950 and 3488 m (Fig. 1 and Table S1). Two core sites, Dome C-Concordia (DC) and Vostok (VK), are located ~ 600 km apart in the central, inner sector of the Plateau, and two, Talos Dome-TALDICE (TD) and GV7, are ~ 200 km apart in peripheral position facing the Ross Sea. They show different modern climate and atmospheric characteristics (e.g., Masson-Delmotte et al., 2011) as well as distance from Quaternary volcanoes of the Antarctic rift province. All the cores used have an undisturbed stratigraphy and are provided with a detailed volcanic aerosol profile, either as sulphate or ECM measurements. They all show the broad and pronounced signal unambiguously related to the AD 1259 event that occurs at variable depth depending on the accumulation rate of the site (between 29.6 m at VK and 181.9 m at GV7, Fig. 1a).

Since at the visual core inspection no macroscopic evidence for the presence of tephra was detected, the core depth intervals corresponding to the volcanic spike were sub-sampled continuously, albeit with different resolution (5–15 cm) depending on the local accumulation rate. Processing of subsamples for laboratory measurements was carried out under clean conditions. To reduce contamination of samples to a minimum, the outer portion of porous firn samples was removed with a clean ceramic knife while ice pieces were washed thrice in ultrapure water. The resulting decontaminated samples were then melted and an aliquot was used for quantitative measurements of dust concentration and size distribution using a Coulter Counter set up in a class 100 clean room (Delmonte et al., 2002) (Fig. 2). The only exception relates to the GV7 core, where presence of abundant drilling fluid prevented accurate Coulter Counter measurements. A separate aliquot of meltwater from levels showing unusually high concentration of particles with respect to the local background was filtered (nucleopore polycarbonate membranes) for tephra recovery. Filters were examined using light and scanning electron microscopes, and typical tephra grains were photographed (Fig. 3). To investigate the source for the recovered material, we determined the major element composition of individual shards using the electron microprobe set up at the Institut des Sciences de la Terre (ISTerre) of Grenoble. The operating details are given in the Supplementary Material.

From the initial geochemical dataset (over 900 analyses) collected during different sessions, we cautiously discarded analytical data showing total oxide sums $\leq$ 60% and those obviously related to pure minerals (quartz, plagioclase, metals, etc.). The rest, consisting of ~320 measurements generally made on very small individual glass particles, was normalised to 100% total oxide values for subsequent interpretation. We expect a decrease of precision but after normalisation all the elements with oxide contents > 1% can be considered robust enough for interpretation (Iverson et al., 2017).

3. Results

EAP core samples selected at the culmination of the volcanic spike show microparticle concentrations well above background levels for each site (Fig. 2). Central Plateau samples show concentrations higher (a factor 6 to 10) than background levels for firn (~8 ppb, Delmonte et al., 2013) and mass size distributions well-defined around modal values smaller than background (~2 μm on average during Holocene, Delmonte et al., 2005). For DC, the mode is around 1.7 μm, while for VK it is between 1.3 μm and 1.9 μm respectively for samples VK-16 and VK-14, although some very large particles up to ~20 μm were observed in the latter.

TD sample 87–1 from the base of the volcanic sulphate peak shows very large particles with mass modal values as high as ~6 μm (Fig. 2), associated with concentration levels higher than ~10 times background levels for firn (~12 ppb, Delmonte et al., 2013). From the lowermost to the uppermost part of the volcanic spike (see Fig. 1a for stratigraphic position of the samples), a progressive

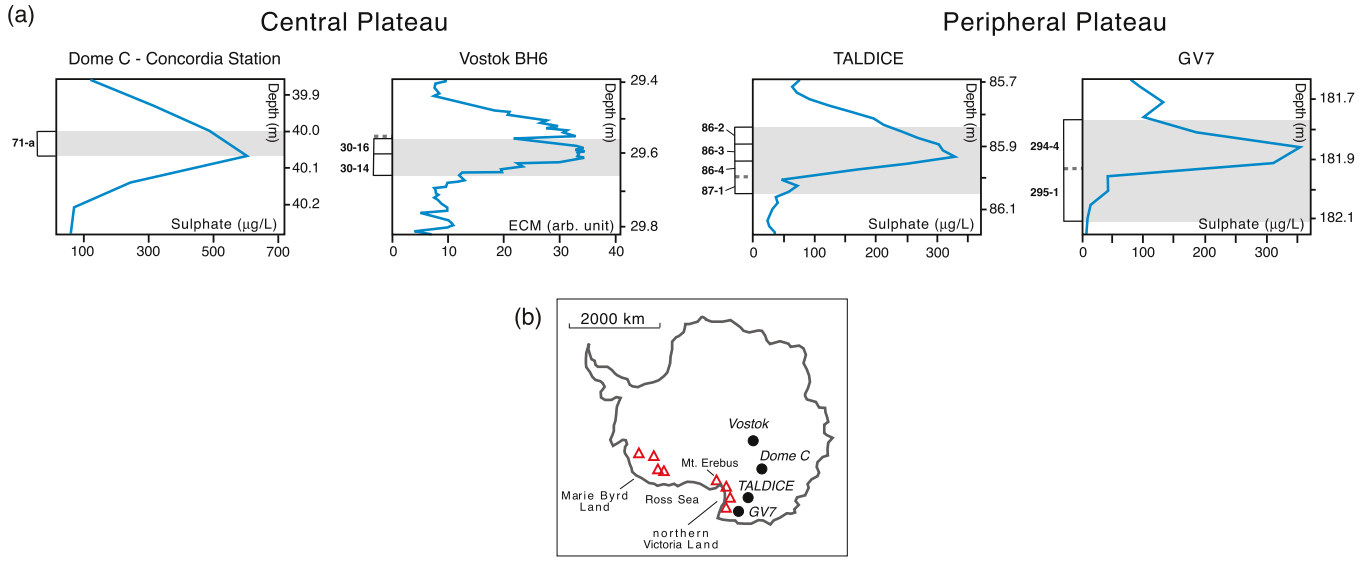

Fig. 1. (a) AD 1259 signal (as sulphate in µg/L, or electrical conductivity, ECM, in arbitrary units) in the studied Antarctic cores. TALDICE sulphate profile redrawn from Severi et al. (2012), GV7 sulphate profile courtesy of R. Nardin. Also shown is the position of samples analysed for grain size and geochemistry (grey shaded blocks). The dashed line indicates 'bag' section limit and/or core break. (b) Map of Antarctica with location of the ice cores and main Quaternary volcanoes in Victoria Land (e.g., Mt. Erebus, Mt. Melbourne and The Pleiades) and in Marie Byrd Land, West Antarctica (e.g., Mt. Takahe and Mt. Berlin).

decrease in microparticle concentration and size can be observed. A population of particles larger than ~5 µm is present in the two deepest samples (TD 87–1 and 86–4), while the relative abundance of particles smaller than 2 µm increases upward within the peak. We note that sample 86-4 shows a bimodal distribution with a first mode smaller than 2 µm and a larger mode around 4–6 µm (Fig. 2).

At the microscopic inspection, glass particles generally display well-preserved textures with no traces of abrasion (Fig. 3) strongly suggesting that the material represents primary un-reworked volcanic ash. Among the examined samples, TD 87–1 and 86–4 contain pumice particles with elongated vesicles up to ca. 40–50 µm long along with fine-size shards remnants of thin vesicle walls. Particles in the filters from the inner EAP cores are typically represented by tiny curved and platy-like shards. Material from sample VK-14 contains glass particles up to 15–20 µm in size. The preserved characteristic morphology of particles coupled with grain size results that indicate both concentrations much higher than background aeolian dust levels and modal values of distributions outside the dust mode (Fig. 2) provide compelling evidence of primary tephra deposition at levels within the AD 1259 acidity peak.

Results of grain-specific geochemical analysis are illustrated in Figs. 4–5, where the data are plotted on the total alkali-silica (TAS) diagram. Silica co-variations with K_2O, CaO, FeO and Al_2O_3, not shown here, are coherent in providing the same chemical pattern. Representative analyses of individual glass shards are presented in Table S3, along with biplot comparisons of selected major-oxide ratios in the present data and in published literature for further potential source volcanoes and equivalents (Supplementary Material).

The analysed glass shards, taken altogether, display variable silica contents, from intermediate to evolved compositions ($SiO_2 > 52$ wt %). No basic and ultrabasic geochemistries are represented. Within the glass heterogeneous composition spreading over three TAS fields, we identify two main separate clusters of data, one trachytic falling in the alkaline field, ~63-65wt %, and the other showing sub-alkaline affinity and straddling the trachyte-dacite-rhyolite boundaries (for brevity referred to hereafter as 'dacitic'), ~70wt %. A third sub-population, subordinate in terms of frequency, shows a siliceous rhyolitic composition ($SiO_2 > 74$ wt %).

Volcanic glass composition also varies spatially (Fig. 4a). Ice core shards from the Central EAP sites are predominantly sub-alkaline in composition. However, the three analysed samples display different characteristics. The very fine-grained DC sample and sample VK-14 also dominantly dacitic. Sample VK-16 displays two clusters of geochemical data. The main glass population is dacitic in composition and appears comparable with that in sample VK-14 and in DC, the subordinate population is a siliceous rhyolite. Sparse analyses from both VK samples fall within the trachytic glass group.

In all six ice sections from the two peripheral EAP sites trachytic tephra particles are dominating, but with occurrence of subordinate glass with different signature (Fig. 4a). At TD, we observe an interesting compositional variation with respect to the time-stratigraphic position of the samples (Fig. 5). Volcanic ash on the TD 87–1 filter, situated at the very beginning of the sulphate fallout (Fig. 1) and containing coarse particles, is mainly trachytic in composition. The adjacent TD 86–4 from the acme of the sulphate volcanic signal shows two main coexisting glass populations. This is consistent with the striking bimodal grain size distribution of this sample (Fig. 2). According to scanning electron microscopic check during microprobe analysis, coarser particles correspond to trachyte, finer particles are mostly dacitic. Glass from the upper TD 86 samples −3 and −2, stratigraphically located at the later part of the spike and populated by fine particles, is trachytic. GV7 ice shows co-existing trachytic and dacitic geochemistries (Fig. 4a). The two analysed samples are equally heterogeneous (not shown). In all samples from the peripheral cores, only one shard from TD falls within the rhyolite cluster identified in VK-16 (Fig. 4a).

4. Interpretation and discussion

4.1. Identification of tephra sources

Filters from all studied cores contain significant volcanic glass that appears heterogeneous both in grain size and geochemistry and present variable spatial characteristics.

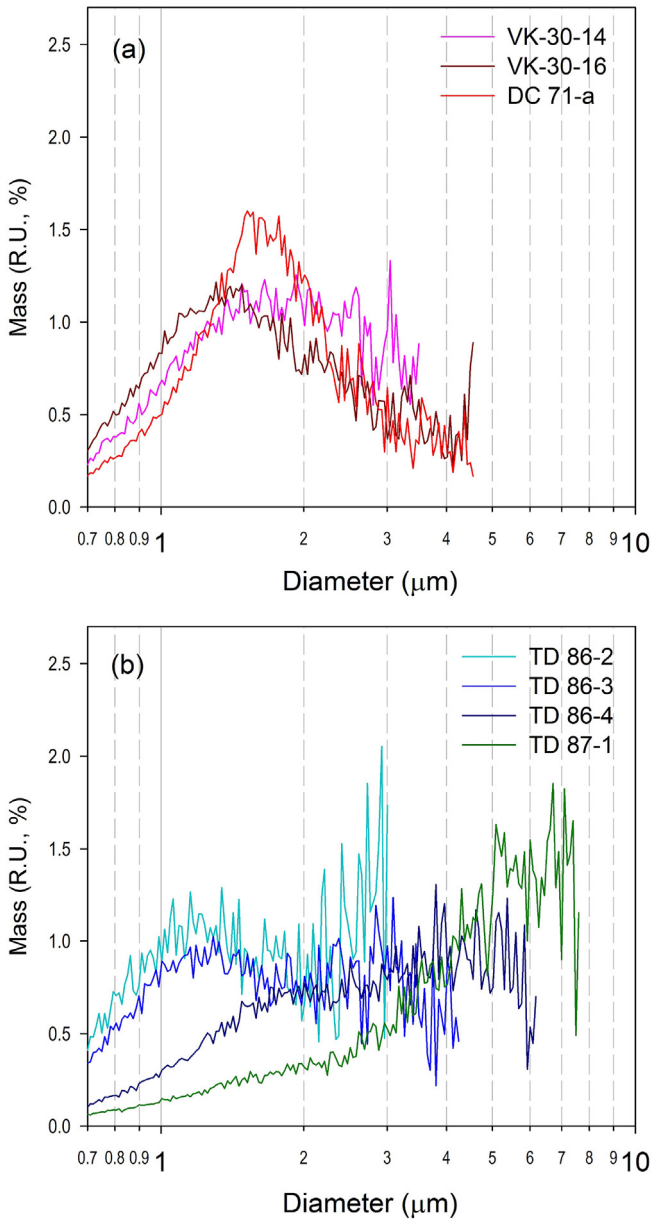

Fig. 2. Mass-size distributions (Relative Units, R.U., %) of samples analysed for geochemistry. (a) Central EAP samples from Dome C (DC 71-a) and Vostok BH6 (VK-30-14 and VK-30-16) ice cores. (b) TD samples 87–1, 86–4, 86–3, 86–2 from the base to the top of the volcanic sulphate spike.

Taken as a whole, the composition of glass shards allows two prevailing and a third subsidiary populations to be distinguished. Trachytic shards are more abundant in the samples from peripheral EAP sites, which are characterised by coarser grain size. Dacitic shards occur in all sites but are dominating in the Central EAP samples, typically characterised by smaller particle size. This pattern already suggests that tephra transport and deposition could be controlled by different atmospheric dynamics over the Plateau. Although tephra transport is very different from background dust input onto the EAP (Narcisi et al., 2005), mineral dust investigations highlighted that the periphery of the ice sheet in fact is influenced by regional atmospheric circulation dynamics of the Western Ross Sea, while sites from the inner part of the EAP are more sensitive to long-range high-altitude transport above Antarctica (e.g., Delmonte et al., 2013).

Focusing on the geochemical signature of volcanic glass as a major criterion for source identification, we first point out that compositional heterogeneity in a tephra horizon could be related to magmatic differentiation during a single parent explosive episode or to coeval deposition from separate events. Several examples of both types of tephra are known in Antarctic ice (e.g., Narcisi et al., 2016). Since alkaline (i.e. trachytic) composition and sub-alkaline (i.e. dacitic) composition typically pertain to different tectonic settings, here we interpret co-existing trachytic and dacitic tephras in the studied samples as related to contemporaneous eruptions from independent sources.

The identified trachytic glass shards are particularly copious in the filters from TD and GV7 peripheral cores. The typical coarse grain size of the trachytic glass suggests that the source area should be located within the South polar region. We eliminate Antarctic sources not including trachytes among their products, i.e. the volcanic centres in the northern Antarctic Peninsula (Moreton and Smellie, 1998; Kraus et al., 2013), the South Sandwich Islands (Nielsen et al., 2007), the Balleny Islands, off the coast of Victoria Land (Green, 1992), Amsterdam-St. Paul and Crozet Islands located in the southern Indian Ocean (Doucet et al., 2004; Breton et al., 2013). Kerguelen, in southern Indian Ocean, erupted trachytes but the last major eruptive event has an age of ~26 ka (Gagnevin et al., 2003). The active stratovolcano of Mt. Erebus, Ross Island (Fig. 1b), is also excluded because is characterised by phonolitic products throughout the last few tens of ka (Iverson et al., 2014). Alkaline trachytic compositions are characteristic of volcanoes within the Antarctic continent associated with the West Antarctic Rift System, one of the largest active rift systems of the world (Rocchi et al., 2002; Panter et al., 2018). In particular, trachytic products occur in northern Victoria Land at Mt. Melbourne, The Pleiades and Mt. Rittmann (e.g., Giordano et al., 2012). These volcanoes are located within a radius of ~250 km from TD and GV7 core sites (Fig. 1b) and represent the source for many tephra layers in these ice cores including the ash horizon dated as AD 1254 ± 2 (Narcisi and Petit, 2019). Trachytes occur also in the more distant Marie Byrd Land (MBL) volcanoes, West Antarctica (Fig. 1b), particularly at the very active Mt. Berlin and Mt. Takahe (Wilch et al., 1999; Dunbar et al., 2008) (Fig. 1b). Although tephra products from MBL volcanoes could potentially reach the East Antarctic ice sheet, the ages of the youngest known eruptions (10.5 ± 2.5 and 8.2 ± 5.4 ka, Wilch et al., 1999; Dunbar et al., 2008) suggest that the activity of these volcanoes is apparently too old for producing our trachytic glass. This chronological argument, along with the geochemical consistency with compositions of the tephra layers in the TALDICE core originated from local sources during the last climatic cycle (Narcisi et al., 2012, 2016, 2017) (Fig. 4b), lead us to deduce that the trachytic glass in the studied samples was produced by a northern Victoria Land explosive eruption at AD 1259.

This event dispersed material mostly over the coastal ice sheet region, but the ash deposition involved also more inland areas of the EAP, as the occurrence of sporadic trachytic shards in the VK samples demonstrates. Infrequent ash layers of Antarctic derivation in long cores from the EAP have been already observed within the last four glacial-interglacial cycle ice series (e.g., Narcisi et al., 2010). We infer that the Antarctic volcanic plume entered into the polar vortex circulation and then rapidly reached the inner sectors of the Plateau. Based on the available data, it is unclear whether the plume from the AD 1259 Antarctic eruption dispersed particulate material onto the SP area. In the early tephra investigation by Palais et al. (1992), no trace of trachytic glass is reported for the Antarctic ice core. That tephra study however, was based upon the analysis of a handful of volcanic particles, representing a limitation for the detection of compositional heterogeneity and multiple fingerprints within individual horizons. Finally, similarly to other local

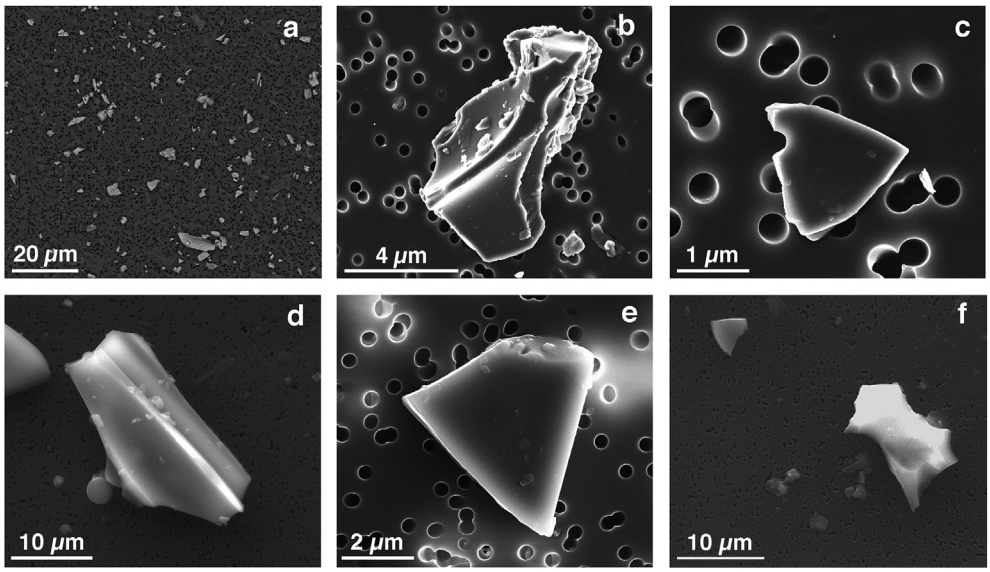

Fig. 3. Scanning electron microphotographs of volcanic glass particles from a, DC-71a; b-c, VK-14; d-e, TD-87-1; f, TD-86-4.

eruptions, this Antarctic event likely delivered sulphate aerosols, but this is difficult to detect as it is combined with the coincidental broad signal peaking at AD 1259 related to long-range stratospheric transport and deposition of aerosols and generated during an extra-Antarctic source event (see discussion below). Note that examples of circa-coeval multiple eruptions manifesting as a single volcanic signal are known in the Antarctic ice record (Cole-Dai and Mosley-Thompson, 1999; Cole-Dai et al., 2000). They represent tricky case studies for estimation of atmospheric aerosol loadings by related eruptions, with implications for assessment of the real impact on climate (e.g., Timmreck et al., 2009).

Our discovery of Antarctic-sourced tephra associated with the AD 1259 acidic deposition is remarkable given the postulated tropical source of the eruption responsible for this polar signal (e.g., Sigl et al., 2015). Nevertheless it is not particularly surprising considering that Antarctic volcanoes from Victoria Land and Marie Byrd Land show evidence of Holocene-historical activity and ice cores drilled adjacent to volcanoes contain numerous locally derived discrete tephra layers, sometimes in the form of invisible horizons, as a result of persistent explosive activity (e.g., Dunbar et al., 2003; Kurbatov et al., 2006; Narcisi et al., 2012). In this respect, we point out that the local eruption identified here does not correspond to the Antarctic event dated 1254 ± 2 AD that produced widespread tephra deposition over most of the Pacific-facing sector of Antarctica (Narcisi and Petit, 2019, and references therein). At TD and GV7 in fact this eruption occurs as both coarse visible ash and a sharp sulphate spike standing well above the background values and clearly preceding the AD 1259 volcanic peak (e.g., Narcisi et al., 2001; Severi et al., 2012). The newly identified event neither corresponds to the local eruption at AD 1261 detected as both volcanic sulphate deposition and a large particle concentration peak in the West Antarctic Ice Sheet (WAIS) Divide ice core (Koffman et al., 2013) that clearly follows the AD 1259 signal. Therefore, within a decade three distinct local events took place in the Antarctic mainland that left tangible fallout traces in the ice sheet. Such rapid succession of eruptions could be overlooked in low time resolution studies and instead needs to be carefully considered when addressing the attribution of Antarctic ice-core signals, as having implications for reconstructions of volcanic forcing.

The main sub-alkaline component of dacitic composition is genetically linked to subduction-related volcanism. Differently from the trachytic glass, it is not straightforward to identify the source responsible for this tephra. The distant geographic location of the EAP with respect to subduction provinces provides no clues, and the tiny particle size of the volcanic material in the Central EAP ice suggests long-distance transport, thus enlarging the suite of potential source areas to be considered to the whole Southern Hemisphere and even beyond the Equator. Note in this respect that although not very frequently, ash produced in equatorial-tropical volcanoes could have reached Antarctica during past eruptions, as in the case of Pinatubo (15°14′N) tephra (2–10 μm) identified in the 1993-94 snow layers at South Pole after the 1991 eruption (Cole-Dai et al., 1997). In the search for possible sources for the dacitic tephra, we therefore considered an extended inventory of volcanoes. A thorough discussion of this piece of our work is presented in Supplementary Material.

The recently discovered volcanic eruption of Samalas in the Indonesian Archipelago (8°33′S) was suggested as the most probable source for the AD 1259 polar spike, due to its exceptional size (estimated VEI and maximum plume height 7 and 43 km, respectively) and appropriate date (e.g., Lavigne et al., 2013; Vidal et al., 2015, 2016; Alloway et al., 2017). Indeed, we found a positive chemical match with Samalas products over all constituent elements considered (Fig. 4b). Thus, the striking geochemical similarities between the Samalas glass and the ice core dacitic glass population along with the significant differences between the ice core glass and products from other potential sources (Fig. S2) led us to conclude that our dacitic glass material was sourced from the Samalas AD 1257 eruption. Note that this volcanic material is also chemically coherent with glass shards formerly found in Greenland and SP ice cores (Palais et al., 1992) suggesting a common source eruption (Fig. 4b). The cataclysmic AD 1257 Samalas explosive eruption clearly ranks among the greatest volcanic events of the Holocene. Once injected into the stratosphere up to about 40 km (Vidal et al., 2015), the Samalas tephra particles must have been transported poleward. Volcanic particles are supposed to settle in the lower stratosphere and accumulate just above the tropopause, similarly to ^{10}Be and sulphate. Then, when stratosphere/troposphere exchange of mass and chemical species occurs above Antarctica, sedimentation of volcanic aerosols proceeds within the troposphere and onto the ice sheet surface. The whole process

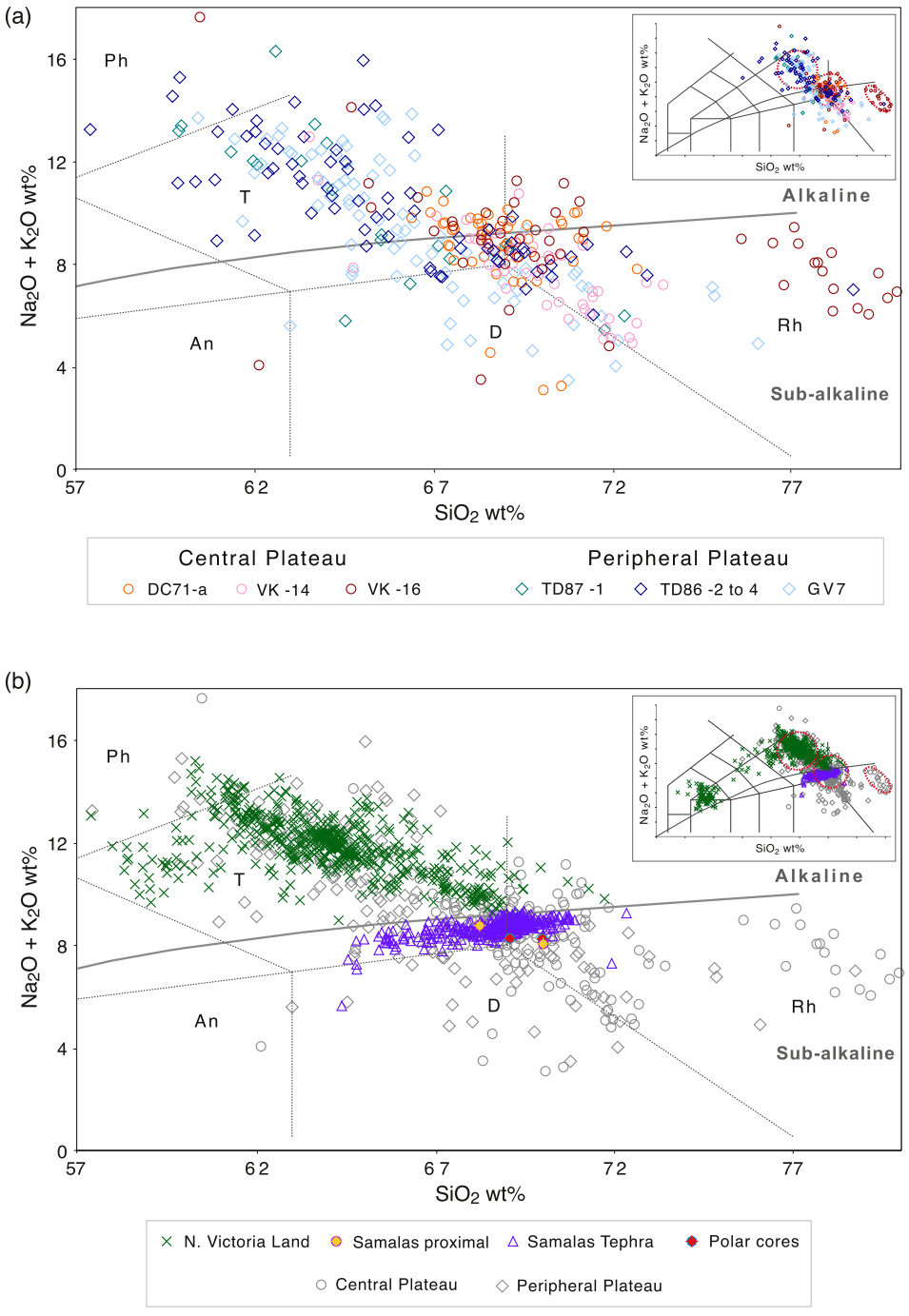

Fig. 4. (a) Total alkali-silica (TAS) classification diagram and alkaline/sub-alkaline division line (Rickwood, 1989, and references therein) showing the normalised analyses of ice-core shards. An = Andesite, D = Dacite, Ph = Phonolite, Rh = Rhyolite, T = Trachyte. The inset shows the TAS diagram with fields (dotted lines) indicating the three major element compositional clusters. (b) The TAS classification diagram as above showing the whole data set (in grey-scale) compared with glass geochemical analyses for the most likely correlatives (data from Alloway et al., 2017; Narcisi et al., 2012, 2016, 2017; Palais et al., 1992). The inset shows the TAS diagram with fields (dotted lines) indicating the three major element compositional clusters. Geochemical comparison with further potential sources is provided in Supplementary Material.

likely occurred on a timescale of 1–2 years, as indicated by the time shift between the eruption and deposition. Evidence for stratospheric transport of volcanic ash to Central EAP in association with strong explosive eruptions is not new. At Vostok, it has been observed (Delmonte et al., 2004) that small particles with modal values around 1.5–1.7 μm are generally associated with stratospheric ash entering the troposphere during stratosphere/troposphere folding, jointly with sulphate and likely ^{10}Be. We believe that in the case of injection of large quantities of volcanic ash to great heights in the stratosphere also some relatively large particles can be transported in the stratosphere at great distance from the source, as suggested by presence of some large dacitic glasses in VK-14 sample.

A limited subset of glass analyses from a Vostok sample indicate distinctive high-silica rhyolitic composition with sub-alkaline affinity. In the TAS diagram, this evolved component appears separated from the two main glass populations previously discussed (insets of Fig. 4), suggesting a different source. Note that this

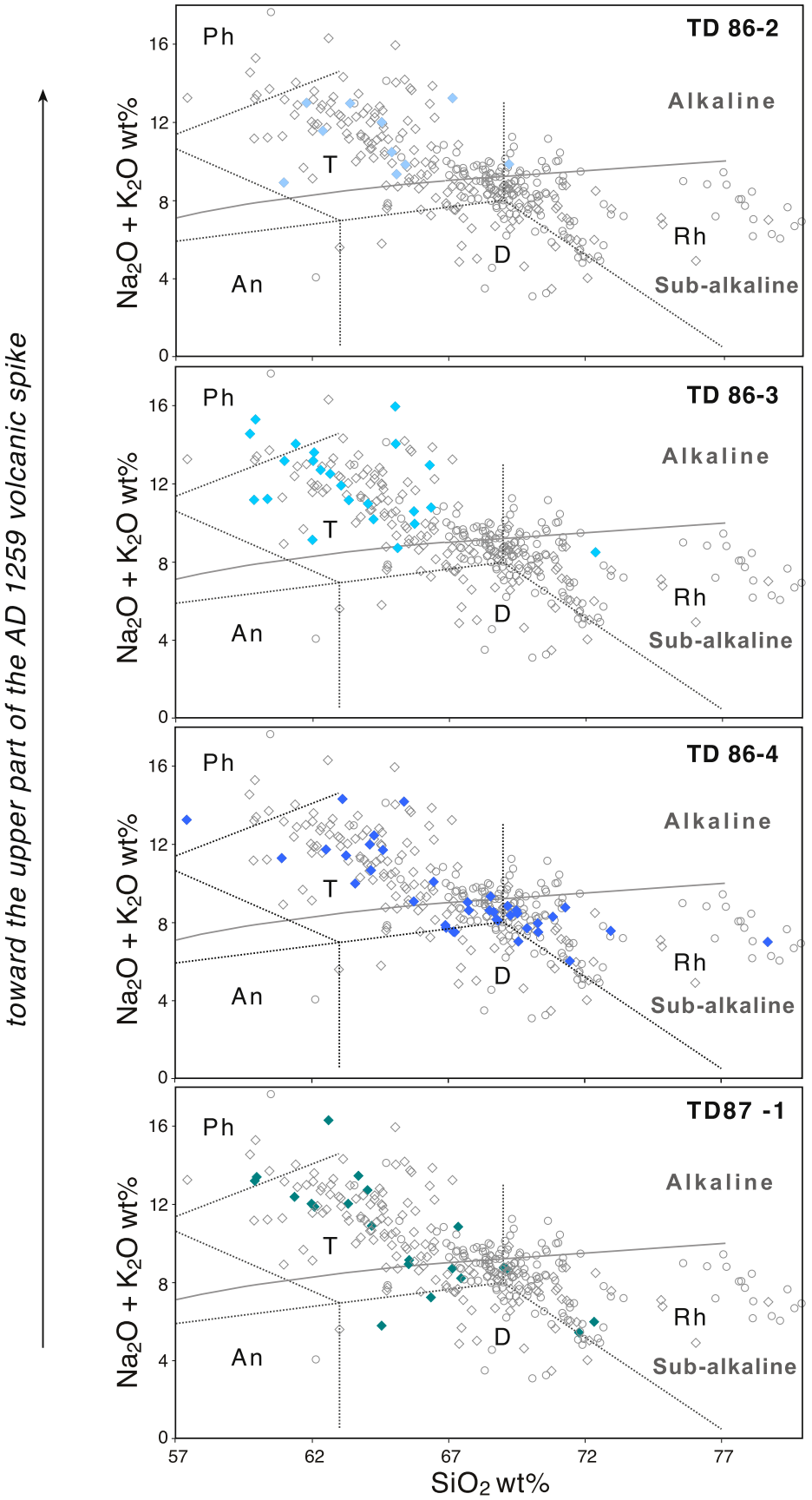

Fig. 5. Total alkali-silica (TAS) classification diagram and alkaline/sub-alkaline division line (Rickwood, 1989, and references therein) for the normalised analyses of ice-core shards in the four TD samples. Data of pertinent samples are superimposed upon the whole data set (in grey-scale) for comparative purposes. An = Andesite, D = Dacite, Ph = Phonolite, Rh = Rhyolite, T = Trachyte. For the stratigraphic position of samples with respect to the AD 1259 ice-core volcanic signal see Fig. 1a.

rhyolitic glass was not detected in the samples from the peripheral sites characterised by conspicuous deposition of locally-originated trachytic ash, suggesting that it is likely unrelated to the newly identified Antarctic eruption. Indeed, no such composition is known in the recent volcanic record from local Antarctic centres (Giordano et al., 2012; Narcisi et al., 2012) and neither in the Samalas products (Vidal et al., 2015; Alloway et al., 2017) (Fig. 4b). We therefore infer that this glass could be originated from a further distant event that contributed to the ice-core tephra. Interestingly, this interpretation could be in accordance with previous investigations in the WAIS Divide ice core that show that the stratospheric microparticle deposition during the year 1258 occurred in two pulses (Koffman et al., 2013), thus hinting for the possible contribution of two quasi-coeval tropical volcanic eruptions.

In the Southern Hemisphere, rhyolitic products related to subduction processes occur at some active Andean volcanoes and especially in the volcanic centres of New Zealand (~39°S, ca. 6000 km from the Vostok site in direct line). Rhyolites rarely occur in the Antarctic volcanoes and, besides, these are not so silicic as the identified rhyolitic glass shards (e.g., Dunbar et al., 2008; Dunbar and Kurbatov, 2011; Kraus et al., 2013). Our rhyolitic glass displays higher K_2O contents compared to glasses of South and Central American contemporary volcanoes; they are also characterised by CaO and FeO contents < 1 wt%, more typical of New Zealand rhyolitic glasses than of the Marie Byrd Land ones found interbedded with Plio-Pleistocene marine sediments (Shane and Froggatt, 1992) (Fig. S3). Although we are aware that some Andean centres may have been more geochemically evolved than is currently represented in literature data, none of the considered volcanoes appear compositionally similar to our ice-core tephra sub-population (Fig. S3).

Considering the recent tephra record of New Zealand volcanoes, we observe that ice-core glass mimics the chemical composition of Kaharoa Tephra, which represents the only rhyolitic deposit during the last 1000 years in the region (Nairn et al., 2004; Lowe et al., 2013) (Fig. S3). This plinian eruption however is precisely dated to AD 1314 ± 12 (Lowe et al., 2013, and references therein), thus is ca. 50 years younger than the polar spike (Lowe and Higham, 1998). Therefore, despite the geochemical similarities, the significant age difference prevents this correlation. We conclude that the source for the identified rhyolitic glass, likely located outside the Antarctic continent, remains undecided. Nevertheless, the New Zealand volcanic province represents the most frequently active rhyolitic zone on Earth (e.g., Smith et al., 2005; Lowe et al., 2013) and is a suitable source of tephra in Antarctica, despite only one New Zealand tephra layer in Antarctic ice has been identified so far (Dunbar et al., 2017). Our intriguing finding could hopefully provide a hint for future investigations.

4.2. Implications

Volcanic eruptions are drivers of transient weather and climate disturbances (e.g., Robock, 2000). The possible climate-forcing produced by the Samalas event, the most powerful eruption of the last millennium, has been addressed in several papers using various proxy archives and historical documents, along with estimate of the release of gas during the eruption based upon an independent geochemical approach. The volatile emissions standing as the greatest volcanogenic gas injection of the last few millennia were enough to produce global cooling (Vidal et al., 2016). Indeed, considerable environmental and social post-volcanic effects were reconstructed that along the Central Indonesian archipelago affected also vast regions of Europe (Alloway et al., 2017; Guillet et al., 2017). According to Gennaretti et al. (2014), tree-ring-based temperature reconstruction from northeastern North America displays an abrupt cooling regime shift that chronologically coincides with the occurrence of a series of eruptions centred around the AD 1257 Samalas event suggesting volcanic impact on the local forests and ice-caps. Moreover, indirect geological sources show occurrence of an El Nino-like event in the Americas and SE Asia in the year after the mega-eruption that suggests a causal connection between the volcanic event and the climate anomaly (Emile-Geay et al., 2008; Alloway et al., 2017). In the Antarctic record, the 13th century appears exceptionally rich in conspicuous volcanic signals, with the AD 1259 being the most prominent (e.g., Cole-Dai et al., 2000). Possible effects of volcanic activity around the date of 1259 have been invoked also for high southern latitudes, but the data are still very sparse. Using a combination of firn/ice core records, Frezzotti et al. (2013) identified middle 13th century as the onset of a 50yrs-long period of negative surface mass balance of the Antarctic ice sheet at the continental scale. This pattern could be related to various superimposing factors, such as solar irradiance and volcanic forcing (Frezzotti et al., 2013).

Results of ice-core tephra studies presented here and elsewhere (Koffman et al., 2013; Narcisi and Petit, 2019, and references therein) collectively have shown for the first time that three distinct Antarctic eruptive episodes took place in the time span of a decade between AD 1254 ± 2 and AD 1261. These eruptions produced deposition of tephra blanket and atmospheric sulphate aerosols onto the polar ice sheet. In the ice volcanic record local eruptions typically emitting only tropospheric sulphate are represented by strong but short-lived residence times of aerosols in the atmosphere (e.g., Castellano et al., 2005). This pattern suggests that such individual events most likely are incapable of significant large-scale climatic impact. However, here we raise the question about the potential consequences of this closely spaced local eruption sequence, which occurred in association with the tropical Samalas eruption, on the Antarctic climate and environment. Note that owing to the close proximity to the source region the local forcing would be exerted through both the radiative impacts of gas and particulate aerosols and the effects on ice surface albedo produced by repeated extensive tephra deposition. With respect to the latter factor, we point out that tephra on ice has a variable impact on melting. Recent estimations have shown the significance of volcanic ash deposition onto snow/ice even from mid-sized eruptions at high-latitudes to alter surface reflectivity and can enhance glacier melting over the area of ash deposition (e.g., Dadic et al., 2013; Young et al., 2014; Muschitiello et al., 2017). However, the effect of the volcanic deposition on snow/ice ablation depends on the thickness of ash deposited and ablation is even deterred where the ash blanket is greater than ~ 2 cm (Driedger, 1981). In this respect surface winds blowing on the ice sheet at the time of the eruption appear also important as could redistribute (i.e. accumulate or disperse) the volcanic material, thereby affecting the local radiative impact. We conclude that given the continuous sustained explosive activity of the Antarctic volcanoes with related large production of tephra and consequent dispersal over the Plateau due to favourable atmospheric conditions (e.g., Scarchilli et al., 2011), we believe that the potential role of forcing caused by locally-derived ash deposits should not be neglected in Antarctic palaeoclimate reconstructions. This factor deserves further more specific investigation in future research.

With respect to sulphate emission, unfortunately the available data currently do not permit to distinguish between the contribution to the aerosol deposition from the Samalas event and the AD 1259 local Antarctic eruption. These limitations notwithstanding, at this stage we can remark that in Antarctica two distinct volcanic forcings (one tropical and the other of high southern-latitude) may be superimposed around the date of 1259. In conclusion, our results

add complexity to interpretation of volcanic aerosol yields from polar records and could have implications for more reliable climate model simulations for the pre-instrumental period (Schneider et al., 2009; Stoffel et al., 2015, and references therein).

5. Conclusions

Non-visible tephra deposits trapped within polar snow and ice represent precious chronostratigraphic tools. When the material is found associated with a prominent acidic signal, firm attribution to specific eruptions can be given with implications for climate forcing reconstructions. However, tephra detection and fingerprinting in such remote locations is often problematic. We successfully used four cores collected from geographically widely separated different sites in the EAP to demonstrate extensive deposition of volcanic dust on the ice sheet coeval with the large acidity peak at AD 1259, a key time stratigraphic horizon of inter-hemispheric significance. Our compelling data show that the material displays different characteristics from site to site. Geochemical fingerprinting of tephra, obtained with a grain-specific methodology, indicates that altogether multiple distinct explosive events have contributed to the ice core ash deposition, i.e. a newly-identified Antarctic eruption in AD 1259, the great AD 1257 eruption of Samalas, and a further eruption likely occurred somewhere outside Antarctica. The spatially-variable deposition of the three distinct tephra populations is related to the different atmospheric circulation patterns influencing the inner sector of the Plateau and sites in peripheral position. This aspect should not be discounted in order to obtain sound source attribution of volcanic signals in polar sequences. We therefore underline the need of detailed studies based upon a multi-site and parameter approach as well as a large number of chemical analyses for capturing complexities inside tephra. Our results of the chemical composition of hundreds of microscopic particles confirm the inferred linkage of the Antarctic ice signal with the Samalas tropical eruption occurred in AD 1257, but also provide evidence for a coincidental cluster of local explosive events, so far not adequately considered in climate reconstructions derived by ice-core volcanic aerosol records. Local activity instead was important in shaping the Antarctic volcanic record and should be regarded as an agent of potential regional disturbances, not least through dispersion of ash over large areas with consequent radiative impact. We emphasise the potential of tephra investigations with respect to traditional measurements of aerosol concentrations in ice also for identifying superimposition of distinct contemporary events at a single site. Our findings also contribute to a more complete reconstruction of the history of volcanic activity in the Antarctic region.

Acknowledgements

We thank D.J. Lowe (University of Waikato) for his useful advice on New Zealand tephrochronology, N. Metrich and J.–C. Komorowski (Institut de Physique du Globe de Paris) for providing tephra samples from the Samalas deposits, C. Rado for drilling operations at Vostok, and E. Gautier (IGE, Grenoble) for DC ice sample selection. We appreciate the constructive comments and valuable advice of J.L. Smellie and an anonymous reviewer. The Vostok ice core was obtained during 1991–92 field season through the Russian US French collaboration on ice cores with the support from the Soviet-Russian Antarctic Expedition, the National Science Foundation and the French Polar Institute. This work contributes to TALos Dome Ice CorE (TALDICE), a joint European programme lead by Italy and funded by national contributions from Italy, France, Germany, Switzerland and the United Kingdom, that was aimed at retrieving an ice core reaching back through the previous two interglacials (about 250,000 years). This is TALDICE publication no 55. The GV7 drilling project, carried out in cooperation with KOPRI (Korean Polar Research Institute), was financially supported by the MIUR (Italian Ministry of University and Research)–PNRA (Italian Antarctic Research Programme) program through the IPICS-2kyr-It project. Author Contributions: B.N. and J.R.P. conceived this study. J.R.P. conducted ice-core sample processing, grain-size analysis, and preliminary microprobe work. B.N. conducted tephra analysis, interpreted the results, and wrote most of the manuscript. V.B. was responsible for microprobe work. B.D. interpreted grain-size data and significantly contributed to the writing of the text. J.S. collaborated in the discussion of the experimental results.

Appendix A. Supplementary data

Supplementary data to this chapter can be found online at https://doi.org/10.1016/j.quascirev.2019.03.005.

References

Alloway, B.V., Andreastuti, S., Setiawan, R., Miksic, J., Hua, Q., 2017. Archaeological implications of a widespread 13th Century tephra marker across the central Indonesian Archipelago. Quat. Sci. Rev. 155, 86–99. https://doi.org/10.1016/j.quascirev.2016.11.020.

Barbante, C., Kehrwald, N.M., Marianelli, P., Vinther, B.M., Steffensen, J.P., Cozzi, G., Hammer, C.U., Clausen, H.B., Siggaard-Andersen, M.-L., 2013. Greenland ice core evidence of the 79 AD Vesuvius eruption. Clim. Past 9, 1221–1232. https://doi.org/10.5194/cp-9-1221-2013.

Baroni, M., Savarino, J., Cole-Dai, J., Rai, V.K., Thiemens, M.H., 2008. Anomalous sulfur isotope compositions of volcanic sulfate over the last millennium in Antarctic ice cores. J. Geophys. Res.: Atmospheres 113 (D20), 2156–2202. https://doi.org/10.1029/2008JD010185.

Breton, T., Nauret, F., Pichat, S., Moine, B., Moreira, M., Rose-Koga, E.F., Auclair, D., Bosq, C., Wavrant, L.-M., 2013. Geochemical heterogeneities within the Crozet hotspot. Earth Planet. Sci. Lett. 376, 126–136.

Castellano, E., Becagli, S., Hansson, M., Hutterli, M., Petit, J.R., Rampino, M.R., Severi, M., Steffensen, J.P., Traversi, R., Udisti, R., 2005. Holocene volcanic history as recorded in the sulfate stratigraphy of the European Project for Ice Coring in Antarctica Dome C (EDC96) ice core. J. Geophys. Res. 110, D06114. https://doi.org/10.1029/2004JD005259.

Cole-Dai, J., Mosley-Thompson, E., 1999. The Pinatubo eruption in South Pole snow and its potential value to ice-core paleovolcanic records. Ann. Glaciol. 29, 99–105. https://doi.org/10.3189/172756499781821319.

Cole-Dai, J., Mosley-Thompson, E., Thompson, L.G., 1997. Quantifying the Pinatubo volcanic signal in south polar snow. Geophys. Res. Lett. 24, 2679–2682.

Cole-Dai, J., Mosley-Thompson, E., Wight, S.P., Thompson, L.G., 2000. A 4100-year record of explosive volcanism from an East Antarctica ice core. J. Geophys. Res. 105 (D19), 24431–24441. https://doi.org/10.1029/2000JD900254.

Dadic, R., Mullen, P.C., Schneebeli, M., Brandt, R.E., Warren, S.G., 2013. Effects of bubbles, cracks, and volcanic tephra on the spectral albedo of bare ice near the Transantarctic Mountains: implications for sea glaciers on Snowball Earth. J. Geophys. Res.: Earth Surface 118, 1658–1676. https://doi.org/10.1002/jgrf.20098.

Delmas, R.J., Kirchner, S., Palais, J.M., Petit, J.R., 1992. 1000 years of explosive volcanism recorded at the South Pole. Tellus 44B, 335–350.

Delmonte, B., Petit, J.R., Maggi, V., 2002. Glacial to Holocene implications of the new 27000-year dust record from the EPICA Dome C (East Antarctica) ice core. Clim. Dyn. 18, 647–660. https://doi.org/10.1007/s00382-001-0193-9.

Delmonte, B., Petit, J.R., Andersen, K.K., Basile-Doelsch, I., Maggi, V., Lipenkov, V.Ya, 2004. Dust size evidence for opposite regional atmospheric circulation changes over east Antarctica during the last climatic transition. Clim. Dyn. 23 (3–4), 427–438.

Delmonte, B., Petit, J.R., Krinner, G., Maggi, V., Jouzel, J., Udisti, R., 2005. Ice core evidence for secular variability and 200-year dipolar oscillations in atmospheric circulation over East Antarctica during the Holocene. Clim. Dyn. 24 (6), 641–654.

Delmonte, B., Baroni, C., Andersson, P.S., Narcisi, B., Salvatore, M.C., Petit, J.R., Scarchilli, C., Frezzotti, M., Albani, S., Maggi, V., 2013. Modern and Holocene aeolian dust variability from Talos Dome (northern Victoria Land) to the interior of the antarctic ice sheet. Quat. Sci. Rev. 64, 76–89. https://doi.org/10.1016/j.quascirev.2012.11.033.

Doucet, S., Weis, D., Scoates, J.S., Debaille, V., Giret, A., 2004. Geochemical and Hf–Pb–Sr–Nd isotopic constraints on the origin of the Amsterdam–St. Paul (Indian Ocean) hotspot basalts. Earth Planet. Sci. Lett. 218, 179–195.

Driedger, C., 1981. Effect of ash thickness on snow ablation. In: Lipman, P.W., Christiansen, R.L. (Eds.), The 1980 Eruptions of Mount St. Helens, Washington, U.S. Geological Survey Prof. Pap. 1250, pp. 757–760.

Dunbar, N.W., Kurbatov, A.V., 2011. Tephrochronology of the Siple Dome ice core, West Antarctica: correlations and sources. Quat. Sci. Rev. 30, 1602–1614.

https://doi.org/10.1016/j.quascirev.2011.03.015.
Dunbar, N.W., Zielinski, G.A., Voisin, D.T., 2003. Tephra layers in the Siple Dome and Taylor Dome ice cores, Antarctica: sources and correlations. J. Geophys. Res. 108 (B8), 2374. https://doi.org/10.1029/2002JB002056.
Dunbar, N.W., McIntosh, W.C., Esser, R.P., 2008. Physical setting and tephrochronology of the summit caldera ice record at Mount Moulton, West Antarctica. Geol. Soc. Am. Bull. 120, 796–812. https://doi.org/10.1130/B26140.1.
Dunbar, N.W., Iverson, N.A., Van Eaton, A.R., Sigl, M., Alloway, B.V., Kurbatov, A.V., Mastin, L.G., Mc Donnell, J.R., Wilson, C.J.N., 2017. New Zealand supereruption provides time marker for the Last Glacial Maximum in Antarctica. Sci. Rep. 7, 12238. https://doi.org/10.1038/s41598-017-11758-0.
Emile-Geay, J., Seager, R., Cane, M.A., Cook, E.R., Haug, G.H., 2008. Volcanoes and ENSO over the past millennium. J. Clim. 21, 3134–3148.
Frezzotti, M., Scarchilli, C., Becagli, S., Proposito, M., Urbini, S., 2013. A synthesis of the Antarctic surface mass balance during the last 800 yr. Cryosphere 7, 303–319. https://doi.org/10.5194/tc-7-303-2013.
Gagnevin, D., Ethien, R., Bonin, B., Moine, B., Féraud, G., Gerbe, M.C., Cottin, J.Y., Michon, G., Tourpin, S., Mamias, G., Perrache, C., Giret, A., 2003. Open-system processes in the genesis of silica-oversaturated alkaline rocks of the Rallier-du-Baty Peninsula, Kerguelen Archipelago (Indian Ocean). J. Volcanol. Geotherm. Res. 123 (3–4), 267–300. https://doi.org/10.1016/S0377-0273(02)00509-7.
Gennaretti, F., Arseneault, D., Nicault, A., Luc Perreault, L., Bégin, Y., 2014. Volcano-induced regime shifts in millennial tree-ring chronologies from northeastern North America. Proc. Natl. Acad. Sci. 111 (28), 10077–10082. https://doi.org/10.1073/pnas.1324220111.
Giordano, G., Lucci, F., Phillips, D., Cozzupoli, D., Runci, V., 2012. Stratigraphy, geochronology and evolution of the Mt. Melbourne volcanic field (North Victoria Land, Antarctica). Bull. Volcanol. 74, 1985–2005. https://doi.org/10.1007/s00445-012-0643-8.
Green, T.H., 1992. Petrology and geochemistry of basaltic rocks from the Balleny Is, Antarctica. Aust. J. Earth Sci. 39 (5), 603–617. https://doi.org/10.1080/08120099208728053.
Guillet, S., Corona, C., Stoffel, M., Khodri, M., Lavigne, F., Ortega, P., et al., 2017. Climate response to the Samalas volcanic eruption in 1257 revealed by proxy records. Nat. Geosci. 10, 123–128.
Hammer, C.U., 1980. Acidity of polar ice cores in relation to absolute dating, past volcanism, and radio–echoes. J. Glaciol. 25, 359–372. https://doi.org/10.3189/S0022143000015227.
Iverson, N.A., Kyle, P.R., Dunbar, N.W., McIntosh, W.C., Pearce, N.J.G., 2014. Eruptive history and magmatic stability of Erebus volcano, Antarctica: insights from englacial tephra. Geochem. Geophys. Geosyst. 15, 4180–4202. https://doi.org/10.1002/2014GC005435.
Iverson, N.A., Kalteyer, D., Dunbar, N.W., Kurbatov, A.V., Yates, M., 2017. Advancements and best practices for analysis and correlation of tephra and cryptotephra in ice. Quat. Geochronol. 40, 45–55. https://doi.org/10.1016/j.quageo.2016.09.008.
Koffman, B.G., Kreutz, K.J., Kurbatov, A.V., Dunbar, N.W., 2013. Impact of known local and tropical volcanic eruptions of the past millennium on the WAIS Divide microparticle record. Geophys. Res. Lett. 40, 1–5. https://doi.org/10.1002/grl.50822.
Kraus, S., Kurbatov, A., Yates, M., 2013. Geochemical signatures of tephras from quaternary antarctic Peninsula volcanoes. Andean Geol. 40 (1), 1–40. https://doi.org/10.5027/andgeoV40n1-a01.
Kurbatov, A.V., Zielinski, G.A., Dunbar, N.W., Mayewski, P.A., Meyerson, E.A., Sneed, S.B., Taylor, K.C., 2006. A 12,000 year record of explosive volcanism in the siple Dome ice core, west Antarctica. J. Geophys. Res. 111 (D12307) https://doi.org/10.1029/2005JD006072.
Langway, C.C., Clausen, H., Hammer, C., 1988. An inter-hemispheric volcanic time-marker in ice cores from Greenland and Antarctica. Ann. Glaciol. 10, 102–108.
Langway Jr., C.C., Osada, K., Clausen, H.B., Hammer, C.U., Shoji, H., 1995. A 10-century comparison of prominent bipolar volcanic events in ice cores. J. Geophys. Res. 100 (D8), 16241–16247.
Lavigne, F., Degeai, J.-P., Komorowski, J.-C., Guillet, S., Robert, V., Lahitte, P., Oppenheimer, C., Stoffel, M., Vidal, C.M., Surono, Pratomo, I., Wassmer, P., Hajdas, I., Sri Hadmoko, D., de Belizal, D., 2013. Source of the great A.D. 1257 mystery eruption unveiled, Salamas volcano, Rinjani Volcanic Complex, Indonesia. Proc. Natl. Acad. Sci. 110 (42), 16742–16747. https://doi.org/10.1073/pnas.1307520110.
Lowe, D.J., 2011. Tephrochronology and its application: a review. Quat. Geochronol. 6, 107–153. https://doi.org/10.1016/j.quageo.2010.08.003.
Lowe, D.J., Higham, T.F.G., 1998. Hit-or-myth? Linking a 1259 AD acid spike with an Okataina eruption. Antiquity 72, 427–431.
Lowe, D.J., Blaauw, M., Hogg, A.G., Newnham, R.M., 2013. Ages of 24 widespread tephras erupted since 30,000 years ago in New Zealand, with re-evaluation of the timing and palaeoclimatic implications of the Lateglacial cool episode recorded at Kaipo bog. Quat. Sci. Rev. 74, 170–194.
Mann, M.E., Zhang, Z., Rutherford, S., Bradley, R.S., Hughes, M.K., Shindell, D., Ammann, C., Faluvegi, G., Ni, F., 2009. Global signatures and dynamical origins of the little ice age and medieval climate anomaly. Science 326, 1256–1260. https://doi.org/10.1126/science.1177303.
Masson-Delmotte, V., Buiron, D., Ekaykin, A., Frezzotti, M., Gallée, H., Jouzel, J., Krinner, G., Landais, A., Motoyama, H., Oerter, H., Pol, K., Pollard, D., Ritz, C., Schlosser, E., Sime, L.C., Sodemann, H., Stenni, B., Uemura, R., Vimeux, F., 2011. A comparison of the present and last interglacial periods in six Antarctic ice cores. Clim. Past 7, 397–423.
Moreton, S.G., Smellie, J.L., 1998. Identification and correlation of distal tephra layers in deep-sea sediment cores, Scotia Sea, Antarctica. Ann. Glaciol. 27, 285–289.
Muschitiello, F., Pausata, F.S.R., Lea, J.M., Mair, D.W.F., Wohlfarth, B., 2017. Enhanced ice sheet melting driven by volcanic eruptions during the last deglaciation. Nat. Commun. 8, 1020. https://doi.org/10.1038/s41467-017-01273-1.
Nairn, I.A., Shane, P.R., Cole, J.W., Leonard, G.J., Self, S., Pearson, N., 2004. Rhyolite magma processes of the ~AD 1315 Kaharoa eruption episode, Tarawera volcano, New Zealand. J. Volcanol. Geotherm. Res. 131, 265–294. https://doi.org/10.1016/S0377-0273(03)00381-0.
Narcisi, B., Petit, J.R., 2019. Englacial tephras of east Antarctica. In: Smellie, J., Panter, K., Geyer, A. (Eds.), Volcanism in Antarctica: 200 Million Years of Subduction, Rifting and Continental Break-Up. Geological Society, London, Memoirs (in press).
Narcisi, B., Proposito, M., Frezzotti, M., 2001. Ice record of a 13th century explosive volcanic eruption in northern Victoria Land, East Antarctica. Antarct. Sci. 13, 174–181.
Narcisi, B., Petit, J.R., Delmonte, B., Basile-Doelsch, I., Maggi, V., 2005. Characteristics and sources of tephra layers in the EPICA-Dome C ice record (East Antarctica): implications for past atmospheric circulation and ice core stratigraphic correlations. Earth Planet. Sci. Lett. 239, 253–265.
Narcisi, B., Petit, J.R., Delmonte, B., 2010. Extended East Antarctic ice core tephrostratigraphy. Quat. Sci. Rev. 29, 21–27.
Narcisi, B., Petit, J.R., Delmonte, B., Scarchilli, C., Stenni, B., 2012. A 16,000-yr tephra framework for the Antarctic ice sheet: a contribution from the new Talos Dome core. Quat. Sci. Rev. 49, 52–63.
Narcisi, B., Petit, J.R., Langone, A., Stenni, B., 2016. A new Eemian record of Antarctic tephra layers retrieved from the Talos Dome ice core (Northern Victoria Land). Glob. Planet. Chang. 137, 69–78. https://doi.org/10.1016/j.gloplacha.2015.12.016.
Narcisi, B., Petit, J.R., Langone, A., 2017. Last glacial tephra layers in the Talos Dome ice core (peripheral East Antarctic Plateau), with implications for chronostratigraphic correlations and regional volcanic history. Quat. Sci. Rev. 165, 111–126.
Nielsen, S.H.H., Hodell, D.A., Kamenov, G., Guilderson, T., Perfit, M.R., 2007. Origin and significance of ice-rafted detritus in the Atlantic sector of the Southern Ocean. Geochem. Geophys. Geosyst. 8, Q12005. https://doi.org/10.1029/2007GC001618.
Oppenheimer, C., 2003. Ice core and palaeoclimatic evidence for the timing and nature of the great mid-13th century volcanic eruption. Int. J. Climatol. 23, 417–426. https://doi.org/10.1002/joc.891.
Palais, J.M., Germani, M.S., Zielinski, G.A., 1992. Interhemispheric transport of volcanic ash from a 1259 A.D. volcanic eruption to the Greenland and Antarctic ice sheets. Geophys. Res. Lett. 19 (8), 801–804.
Panter, K.S., Castillo, P., Krans, S., Deering, C., McIntosh, W., Valley, J.W., Kitajima, K., Kyle, P., Hart, S., Blusztajn, J., 2018. Melt origin across a rifted continental margin: a case for subduction-related metasomatic agents in the lithospheric source of alkaline basalt, NW Ross Sea, Antarctica. J. Petrol. 59, 517–558. https://doi.org/10.1093/petrology/egy036.
Petit, J.R., Narcisi, B., Batanova, V.G., Savarino, J., Komorowski, J.C., Michel, A., Metrich, N., Besson, P., Vidal, C., Sobolev, A.V., 2016. Identifying the AD 1257 Salamas volcanic event from micron-size tephra composition in two East Antarctic ice cores. Geophys. Res. Abstr. 18, EGU2016–5191.
Ponomareva, V., Portnyagin, M., Davies, S.M., 2015. Tephra without borders: far-reaching clues into past explosive eruptions. Front. Earth Sci. 3 (83) https://doi.org/10.3389/feart.2015.00083.
Rickwood, P.C., 1989. Boundary lines within petrologic diagrams which uses oxides of major and minor elements. Lithos 22, 247–263.
Robock, A., 2000. Volcanic eruptions and climate. Rev. Geophys. 38, 191–219. https://doi.org/10.1029/1998RG000054.
Rocchi, S., Armienti, P., D'Orazio, M., Tonarini, S., Wijbrans, J.R., Di Vincenzo, G., 2002. Cenozoic magmatism in the western Ross embayment: role of mantle plume versus plate dynamics in the development of the West Antarctic rift system. J. Geophys. Res. 107 (B9), 2195. https://doi.org/10.1029/2001JB000515.
Scarchilli, C., Frezzotti, M., Ruti, P.M., 2011. Snow precipitation at four ice core sites in East Antarctica: provenance, seasonality and blocking factors. Clim. Dyn. 37, 2107–2125. https://doi.org/10.1007/s00382-010-0946-4.
Schneider, D.P., Ammann, C.M., Otto-Bliesner, B.L., Kaufman, D.S., 2009. Climate response to large, high-latitude and low-latitude volcanic eruptions in the Community Climate System Model. J. Geophys. Res. 114, D15101. https://doi.org/10.1029/2008JD011222.
Severi, M., Udisti, R., Becagli, S., Stenni, B., Traversi, R., 2012. Volcanic synchronisation of the EPICA-DC and TALDICE ice cores for the last 42 kyr BP. Clim. Past 8, 509–517.
Shane, P.A.R., Froggatt, P.C., 1992. Composition of widespread volcanic glass in deep-sea sediments of the Southern Pacific Ocean: an Antarctic source inferred. Bull. Volcanol. 54, 595–601.
Sigl, M., McConnell, J.R., Toohey, M., Curran, M., Das, S.B., Isaksson, E., Kawamura, K., Kipfstuhl, S., Krüger, K., Layman, L., Maselli, O.J., Motizuki, Y., Motoyama, H., Pasteris, D.R., Severi, M., 2014. Insights from Antarctica on volcanic forcing during the common era. Nat. Clim. Change 4, 693–697. https://doi.org/10.1038/nclimate2293.
Sigl, M., Winstrup, M., McConnell, J.R., Welten, K.C., Plunkett, G., Ludlow, F., Büntgen, U., Caffee, M., Chellman, N., Dahl-Jensen, D., Fischer, H., Kipfstuhl, S., Kostick, C., Maselli, O.J., Mekhaldi, F., Mulvaney, R., Muscheler, R., Pasteris, D.R., Pilcher, J.R., Salzer, M., Schüpbach, S., Steffensen, J.P., Vinther, B.M.,

Woodruff, T.E., 2015. Timing and climate forcing of volcanic eruptions for the past 2,500 years. Nature 523, 543–549. https://doi.org/10.1038/nature14565.
Smith, V.C., Shane, P., Nairn, I.A., 2005. Trends in rhyolite geochemistry, mineralogy, and magma storage during the last 50 kyr at Okataina and Taupo volcanic centres, Taupo Volcanic Zone, New Zealand. J. Volcanol. Geotherm. Res. 148 (3–4), 372–406. https://doi.org/10.1016/j.jvolgeores.2005.05.005.
Stoffel, M., Khodri, M., Corona, C., Guillet, S., Poulain, V., Bekki, S., Guiot, J., Luckman, B.H., Oppenheimer, C., Lebas, N., Beniston, M., Masson-Delmotte, V., 2015. Estimates of volcanic-induced cooling in the northern Hemisphere over the past 1,500 years. Nat. Geosci. 8, 784–788. https://doi.org/10.1038/NGEO2526.
Stothers, R.B., 2000. Climatic and demographic consequences of the massive volcanic eruption of 1258. Clim. Change 45, 361–374.
Svensson, A., Bigler, M., Blunier, T., Clausen, H.B., Dahl-Jensen, D., Fischer, H., Fujita, S., Goto-Azuma, K., Johnsen, S.J., Kawamura, K., Kipfstuhl, S., Kohno, M., Parrenin, F., Popp, T., Rasmussen, S.O., Schwander, J., Seierstad, I., Severi, M., Steffensen, J.P., Udisti, R., Uemura, R., Vallelonga, P., Vinther, B.M., Wegner, A., Wilhelms, F., Winstrup, M., 2013. Direct linking of Greenland and Antarctic ice cores at the Toba eruption (74 ka BP). Clim. Past 9, 749–766. https://doi.org/10.5194/cp-9-749-2013.
Timmreck, C., Lorenz, S.J., Crowley, T.J., Kinne, S., Raddatz, T.J., Thomas, M.A., Jungclaus, J.H., 2009. Limited temperature response to the very large AD 1258 volcanic eruption. Geophys. Res. Lett. 36, L21708. https://doi.org/10.1029/2009GL040083.
Vidal, C.M., Komorowski, J.-C., Metrich, N., Pratomo, I., Kartadinata, N., Prambada, O., Michel, A., Carazzo, G., Lavigne, F., Rodysill, J., Fontijn, K., Surono, 2015. Dynamics of the major plinian eruption of Samalas in 1257 A.D. (Lombok, Indonesia). Bull. Volcanol. 77, 73. https://doi.org/10.1007/s00445-015-0960-9.
Vidal, C.M., Metrich, N., Komorowski, J.-C., Pratomo, Indyo, Michel, A., Kartadinata, N., Robert, V., Lavigne, F., 2016. The 1257 Samalas eruption (Lombok, Indonesia): the single greatest stratospheric gas release of the Common Era. Sci. Rep. 6, 34868. https://doi.org/10.1038/srep34868.
Wilch, T.I., McIntosh, W.C., Dunbar, N.W., 1999. Late Quaternary volcanic activity in Marie Byrd Land: potential $^{40}Ar/^{39}Ar$-dated time horizons in West Antarctic ice and marine cores. Geol. Soc. Am. Bull. 111 (10), 1563–1580.
Yalcin, K., Wake, C.P., Kreutz, K.J., Germani, M.S., Whitlow, S.I., 2006. Ice core evidence for a second volcanic eruption around 1809 in the Northern Hemisphere. Geophys. Res. Lett. 33, L14706. https://doi.org/10.1029/2006GL026013.
Young, C.L., Sokolik, I.N., Flanner, M.G., Dufek, J., 2014. Surface radiative impacts of ash deposits from the 2009 eruption of Redoubt volcano. J. Geophys. Res. Atmos. 119, 11387–11397. https://doi.org/10.1002/2014JD021949.
Zielinski, G.A., 1995. Stratospheric loading and optical depth estimates of explosive volcanism over the last 2100 years derived from the GISP2 Greenland ice core. J. Geophys. Res. 100, 20937–20955. https://doi.org/10.1029/95JD01751.
Zielinski, G.A., Dibb, J.E., Yang, Q., Mayewski, P.A., Whitlow, S., Twickler, M.S., Germani, M.S., 1997. Assessment of the record of the 1982 El Chichón eruption as preserved in Greenland snow. J. Geophys. Res. 102 (D25), 30031–30045. https://doi.org/10.1029/97JD01574.